

# Atomic Physics with the Goddard High Resolution Spectrograph on the *Hubble Space Telescope*.

## V. Oscillator Strengths for Neutral Carbon Lines below 1200 Å<sup>1</sup>

S.R. Federman and J. Zsargó

Department of Physics and Astronomy, University of Toledo, Toledo, OH 43606

### ABSTRACT

We analyzed high resolution spectra of interstellar C I absorption toward  $\lambda$  Ori, 1 Sco, and  $\delta$  Sco that were obtained with the Goddard High Resolution Spectrograph on the *Hubble Space Telescope*. Several multiplets were detected within the wavelength interval 1150 to 1200 Å, where most C I lines have ill-defined oscillator strength; multiplets at longer wavelengths with well-defined atomic parameters were also seen. We extracted accurate column densities and Doppler parameters from lines with precise laboratory-based  $f$ -values. These column densities and  $b$ -values were used to obtain a self-consistent set of  $f$ -values for all the observed C I lines. For many of the lines with wavelength below 1200 Å, the derived  $f$ -values differ appreciably from the values quoted in the compilation by Morton (1991). The present set of  $f$ -values extends and in some cases supersedes those given in Zsargó et al. (1997), which were based on lower resolution data.

*Subject headings:* atomic data - ISM: abundances - ultraviolet: ISM

### 1. Introduction

Accurate oscillator strengths ( $f$ -values) are needed for spectroscopic studies in astronomy. For instance, they are required when extracting reliable abundances from interstellar absorption lines, when modeling opacities in stellar atmospheres, or when utilizing temperature and density diagnostics. While analyzing such spectra from space-borne, high-resolution UV spectrographs, one can encounter the problem that uncertainties associated with observational sources are less than those from atomic physics. This is especially true when the astronomical data have signal-to-noise ratios greater than 100 to 200. One can take advantage of the situation by refining  $f$ -values for lines giving discordant results. The basic premise involves obtaining column densities and Doppler parameters from lines where there is consensus on  $f$ -values and then using this information in refining other  $f$ -values.

---

<sup>1</sup>Based on observations obtained with the NASA/ESA *Hubble Space Telescope* through the Space Telescope Science Institute, which is operated by the Association of Universities for Research in Astronomy, Inc., under NASA contract NAS5-2655.

Several recent studies based on interstellar spectra acquired with the Goddard High Resolution Spectrograph (GHRS) on the *Hubble Space Telescope (HST)* have adopted this methodology. Federman & Cardelli (1995) provided new  $f$ -values for lines of S I; many of their determinations were confirmed by subsequent theoretical (Tayal 1998) and experimental work (e.g., Biemont et al. 1998). Cardelli & Savage (1995) analyzed Fe II lines, and Zsargó, Federman, & Cardelli (1997) refined  $f$ -values for C I lines with central wavelength below 1200 Å as well as for some forbidden lines above this limit. Relative  $f$ -values were derived for singly-ionized nickel (Zsargó & Federman 1998) and singly-ionized cobalt (Mullman et al. 1998). The latter analysis was performed in parallel with laboratory measurements that placed astronomical oscillator strengths on an absolute scale. Laboratory measurements on Ni II by Fedchak, Wiese, & Lawler (2000) validated the relative  $f$ -values in our earlier work on singly-ionized nickel.

In the present paper, following the method outlined in Zsargó et al. (1997), we improved upon their  $f$ -values for C I lines with wavelength below 1200 Å and expand the number of lines in their list. In Section 2 we briefly describe the astronomical measurements available for our analysis, and in Section 3 we discuss how we obtained column densities and Doppler parameters for each absorbing component (3.1) and how we adjusted  $f$ -values (3.2). Finally, we discuss our results in Section 4.

## 2. Measurements

We retrieved observations for  $\lambda$  Ori, 1 Sco, and  $\delta$  Sco from the *HST* archive. Most of the measurements were acquired at medium resolution (MR) and a handful of them were taken at high resolution (HR). These spectra covered several C I multiplets and forbidden lines between 1150 Å and 1700 Å.

The reduction was fairly straightforward, and only minor technical problems arose. The most serious concern was an error in the background correction on some of our preprocessed data. We detected this error on all of our HR spectra containing the  $\lambda 1261$  (UV9) multiplet of C I. The flux level of strongly saturated lines, such as those of S II and Si II, should be zero at line center; however, in some cases we measured negative or small positive values, clearly indicating an erroneous background correction. We could then apply an additional correction to compensate for the effect. The continuum placement turned out to be difficult for some multiplets, due to blending of several lines or simply because the lines were saturated. For example, in the vicinity of multiplet  $\lambda 1261$  in MR spectra, Si II and Fe II lines seriously affected the continuum placement. Following line identification and continuum placement, the Doppler shift (relative to the laboratory wavelength) and equivalent width ( $W_\lambda$ ) of neutral carbon lines were measured. In some cases, only upper limits could be calculated based on the average full width at half maximum (FWHM) of the instrumental function and the root mean square (rms) average of the noise in the stellar continuum.

We now give a brief description of the available spectra for each of our targets and the data reduction done on them. We list the measured  $W_\lambda$  values together with those calculated from

synthetic profiles (see Section 3.1 for details on profile synthesis) and measured in earlier work. We note that the agreement between our  $W_\lambda$  values and those obtained with the *Copernicus* satellite (Jenkins & Shaya 1979; Jenkins, Jura, & Loewenstein 1983) is very good.

### 2.1. $\lambda$ Ori (HD36861)

We retrieved eight observations of  $\lambda$  Ori from the *HST* archive (see Table 1), two at high resolution and six at medium. Both HR spectra, z3di0204t and z3di0205t, were made with the Large Science Aperture (LSA) and so their resolution was slightly lower than usual ( $\approx 4$  km s $^{-1}$  instead of  $\approx 3$  km s $^{-1}$ ). The only observable C I lines in the range of HR spectra were those of the multiplets  $\lambda\lambda 1157$  (UV16), 1158 (UV15.01). There were two additional multiplets covered by the MR observations,  $\lambda 1261$  and  $\lambda 1329$  (UV4). We could measure  $W_\lambda$  for all resolved lines (see Table 2 for measured and calculated values). The two resolved components are separated by  $\approx 12$  km s $^{-1}$ , as seen in Na I D spectra (Hobbs 1974).

### 2.2. 1 Sco (HD141637)

We retrieved eight measurements of 1 Sco from the *HST* archive (Table 1), two at high and six at medium resolution. The HR spectra contained three multiplets,  $\lambda\lambda 1194$  (UV9.02) and 1329 fully and  $\lambda 1193$  (UV11) partially. Multiplet  $\lambda 1329$  was very useful for our analysis, since it has very well established oscillator strengths. In MR spectra, we had measurements of all important multiplets with central wavelength between 1200 Å and 1700 Å [ $\lambda\lambda 1261$ , 1277 (UV7), 1280 (UV5), 1329, 1561 (UV3), and 1657 (UV2)]. The measured and calculated  $W_\lambda$  values, together with earlier measurements, are listed in Table 3. The two components are separated by about 7 km s $^{-1}$  and correspond to the strongest components in Na I D (Welty, Hobbs, & Kulkarni 1994).

### 2.3. $\delta$ Sco (HD143275)

We obtained 7 observations of  $\delta$  Sco, as listed in Table 1, from the *HST* archive. Four of them were high resolution, while the rest were medium resolution. Two of the HR spectra, z3di0504t and z3di0505t, were made with the LSA; hence, their resolution was lower than usual. We could identify most members of the multiplets  $\lambda\lambda 1157$ , 1158 in these observations. The other two HR observations (z34r020dt and z34r020et) were of very good quality. The Small Science Aperture (SSA) was utilized; therefore, they had the maximum possible resolution of the GHRS. Both covered multiplet  $\lambda 1261$  only, close to the upper wavelength end of the spectra, and the  $J=2$  lines were out of the range of z34r020dt. We also had three MR spectra containing the full  $\lambda 1261$  multiplet. A combined MR spectrum was created to increase the signal-to-noise ratio. The measured and calculated  $W_\lambda$  values, together with previous measurements, are given in Table 4. The 5 km s $^{-1}$  separation in components is seen in K I also (Welty & Hobbs 2000) and between the two CH $^+$  components found by Crane, Lambert, & Sheffer (1995).

### 3. Model

#### 3.1. Profile Synthesis

Transitions belonging to the same fine structure level can be characterized by the same column density ( $N$ ), Doppler or line-broadening parameter ( $b$ -value), and Doppler shift. All the other parameters are independent of the line of sight (LOS), and are transition specific. In particular, line oscillator strengths, or  $f$ -values, are needed. Our task was to specify the number of absorbing components and the corresponding column densities and  $b$ -values for all observable fine structure levels.

The number of resolved components, which correspond to the strongest features seen in Na I, K I, and CH<sup>+</sup> spectra, was revealed by visual inspection. There might be, of course, some unresolved ones with separation between them less than the resolution. While slight differences in extracted column densities may result in our approach, the unresolved components could be treated as a single component for all of our modelling purposes.

We had two options to find the column densities and  $b$ -values. The first, a more traditional and simpler way, is the curve of growth (COG) analysis. While it is relatively easy to implement, it is less effective in finding the parameter values, since only the  $W_\lambda$  is used and not the entire line profile. Also, the COG method is not suitable for analyzing blended lines. We used this method only to adjust oscillator strengths, whenever it was necessary or possible to do so [see Zsargó et al. (1997) for details].

We used the more complex and accurate method that matches the observed profiles with synthesized ones to find the LOS-specific parameters. We calculated the “observed” fluxes for all spectra with a given set of column densities, component velocities, and  $b$ -values, and compared them to the corresponding observations. The set of initial parameters then was adjusted until a satisfactory fit could be achieved. The final sets of parameters appear in Table 5 for our lines of sight. Here for simplicity, Doppler shifts are relative to the main velocity component which was set at  $\sim 0$  km s<sup>-1</sup> within IRAF, the Image Reduction and Analysis Facility from the National Optical Astronomy Observatories. The slight differences in velocity between fine structure levels (usually less than  $\pm 0.5$  km s<sup>-1</sup>) for the primary components are small compared to the spectral resolution of  $\approx 3.5$  km s<sup>-1</sup>. The velocities were fixed for the secondary component in each case. Figures 1 and 2 show the observed and synthesized HR spectra of multiplets  $\lambda\lambda 1194$  and  $1329$  for 1 Sco. We used the new oscillator strengths for multiplet  $\lambda 1194$  to produce the synthesized spectrum. Details of the profile synthesis will be presented in another paper (Zsargó, Federman, & Welty 2001).

#### 3.2. Revision of Neutral Carbon Oscillator Strengths

The neutral carbon multiplets and forbidden lines that were used throughout our analysis covered the wavelength range 1150 to 1700 Å. Every multiplet above 1200 Å is thought to have

well established  $f$ -values. Measurements and calculations have been performed, and a general consensus has been achieved about the values (see Morton 1991). However, for the multiplets with wavelengths below 1200 Å and for some weak forbidden lines above it, only calculations are available. The lack of laboratory and precise astronomical measurements make these oscillator strengths less reliable.

The quality of GHRS spectra are generally very good, especially those with high spectral resolution. This provides a unique opportunity to fill in the gap of missing measurements. Consider the situation where HR spectra of two multiplets for a given LOS, one with well defined and the other with poorly defined oscillator strengths, are available. The first multiplet can be used to infer the LOS information, which is then the basis for refining the  $f$ -values for the second multiplet. Obviously, the more spectra of multiplets with well-defined oscillator strengths we possess, the more precise the adjustment will be.

We adjusted oscillator strengths with a curve of growth analysis. The adjustment of ill-defined  $f$ -values is accomplished by placing all  $(f \times \lambda, W_\lambda/\lambda)$  points on the curve by a  $\chi^2$  analysis. A special algorithm, described in detail by Zsargó et al. (1997), was used to accomplish this goal. This algorithm allowed us to adjust the  $f$ -values either individually for each line or as a group for members of the same multiplet. It should be noted that there is danger in such an adjustment. Saturated lines lie on the flat part of the COG, and in such cases, a small uncertainty in  $W_\lambda$  can result in a large error in  $f$ -value. Similar errors can occur if the  $b$ -value is ill defined. This parameter controls where the COG departs from the linear approximation; therefore, bad  $b$ -values can result in considerable errors in the values of the adjusted oscillator strengths. It is important to have very reasonable estimates for  $b$ -values and limit this approach for the weaker lines. While we could not quantify the effect of uncertainties in  $b$ -values, it is reassuring that we were able to get self-consistent results with the adjusted  $f$ -values toward multiple lines of sight (Zsargó et al. 2001).

## 4. Discussion

### 4.1. Reanalysis of J=0 Data for $\beta^1$ Sco

In the course of our work here, we found that Morton's (1991)  $f$ -value for  $\lambda 1276$  yielded more consistent results than the one given by us (Zsargó et al. 1997). Closer inspection of our earlier analysis on  $\lambda 1276$  revealed that this line was on the flat portion of the curve of growth for  $\rho$  Oph A and  $\chi$  Oph, and so its  $f$ -value could not be reliably determined from those data. This supports the inference made by Wannier et al. (1999) from HR spectra of C I in the envelope of the molecular cloud B5. [The other spin-forbidden transitions studied by Zsargó et al. (1997) were weaker and lie on the linear portion of the COG.]

Unfortunately, our analysis of the  $J=0$  lines in the spectrum of  $\beta^1$  Sco was based in large measure on  $\lambda 1276$ . If instead we use the multiplets  $\lambda\lambda 1261, 1329$ , we obtain a column density of  $(1.0 \pm 0.1) \times 10^{14}$  cm $^{-2}$  and a  $b$ -value of 2.3 km s $^{-1}$ . These parameters lead to significant changes

in  $f$ -values for  $J=0$  lines below 1200 Å. The results presented in Table 6 for  $J=0$  are from the revised analysis. Since the  $J=1$  and 2 lines originally were based on  $\lambda\lambda 1261, 1329$ , no changes were made to their  $f$ -values.

#### 4.2. Comparison with Other Results

We adjusted oscillator strengths for several lines and multiplets; they are displayed in Table 6. Both the new values and others are listed, together with the ratios of the  $f$ -values from Morton's (1991) compilation to our new values. The estimated uncertainties for the new oscillator strengths are given within parentheses and are based on the uncertainties in  $W_\lambda$  and a 10% uncertainty in column density, taken in quadrature. The uncertainty in column density is mainly the result of continuum placement. The agreement between the present results for  $J=0$  and those of Zsargo et al. (1997), as corrected above, is generally very good. The differences involving lines in multiplet  $\lambda 1157$  may be caused by the use of MR spectra in our earlier effort. The comparison with the recommended values of Morton (1991) for the multiplets  $\lambda\lambda 1193, 1194$  is also very good, except for the line at 1193.6 Å; the correspondence for lines at shorter wavelengths is less satisfactory. Where significant differences are found, they appear to be the result of a breakdown in LS coupling rules for dipole-allowed transitions. The comparison with the theoretical work of Hibbert et al. (1993) shows that the results are very similar. The agreement with the  $f$ -values given by the compilation of Wiese, Fuhr, & Deters (1996) is good for lines above 1158.5 Å in large measure because they adopted the results of Hibbert et al. (1993). Below this wavelength our results suggest that LS coupling breaks down. For  $\lambda 1193.6$ , where a factor-of-2 difference arises in the  $f$ -value of Welty et al. (1999), it is between ours and Morton's (1991).

The ratios given in the last column are very useful in assessing whether LS coupling applies or not. Since Morton (1991) always assumed LS coupling [and so did Wiese et al. (1996) below 1180 Å], any variation in the ratio within a multiplet indicates that this approximation does not apply. The results of using Cowan's (1981) atomic structure code (Zsargó et al. 1997) can be used as a guide in describing the breakdown of LS coupling rules. As noted by Zsargó et al. (1997), configuration interaction (CI) is stronger in  $\lambda 1194$  ( $5s\ 3P_{0,1,2}^o$ ) than in  $\lambda 1189$  (UV14) and there is CI between  $\lambda 1158$  ( $6s\ 3P_{0,1,2}^o$ ) and  $\lambda 1156$  (UV19) for level  $J=1$ . Another prediction is CI between  $\lambda 1158$  and  $\lambda 1156$  for  $J=2$ , which we confirm now through observational data. We also see the predicted spin-orbit (SO) mixing between  $2s^2\ 2p\ 6s\ 3P_2^o$  and  $2s^2\ 2p\ 5d\ 3D_2^o$  (of  $\lambda 1157$ ). No other strong effects are seen in  $\lambda 1157$ , as predicted.

#### 4.3. Concluding Remarks

In the course of a larger study involving C I excitation (Zsargo et al. 2001), we found that lines below 1200 Å gave inconsistent column densities and  $b$ -values. In the present work, we described refinements to the  $f$ -values for these lines so that a self-consistent analysis was possible. We readjusted the oscillator strengths for some lines in our earlier work (Zsargo et al. 1997)

to correct for the (then) inappropriate choice of  $\lambda 1276$  as the basis of our analysis for the  $J=0$  fine-structure level, and we find good agreement between results from the independent data sets. For the few instances where differences are seen, the current  $f$ -values are preferred because they are based on HR spectra. We also supplemented our inventory of refined  $f$ -values with lines that were not available in our earlier work. The agreement between our and other recent compilations is generally good. Where disagreements arise, they mainly result from the assumption in other work that LS coupling applies for the multiplets  $\lambda\lambda 1157$  and 1158, an approximation not supported by our measurements and analysis. Our extended set of  $f$ -values for C I lines below 1200 Å can be used with confidence in analyses of interstellar spectra acquired with the *Far Ultraviolet Spectroscopic Explorer*.

This research was supported by NASA grant NAG5-7754 and STScI grant AR-08352.01-A.

## REFERENCES

Biemont, E., Garnir, H. P., Federman, S. R., Li, Z. S., & Svanberg, S. 1998, ApJ, 502, 1010

Cardelli, J. A., & Savage, B. D. 1995, ApJ, 452, 275

Cowan, R.D. 1981, Theory of Atomic Structure and Spectra (Berkeley: Univ. California Press)

Crane, P., Lambert, D. L., & Sheffer, Y. 1995, ApJS, 99, 107

Fedchak, J. A., Wiese, L. M., & Lawler, J. E. 2000, ApJ, 538, 773

Federman, S. R., & Cardelli, J. A. 1995, ApJ, 452, 269

Hibbert, A., Biemont, E., Godefroid, M., & Vaeck, N. 1993, A&AS, 99, 179

Hobbs, L. M. 1974, ApJ, 191, 381

Jenkins, E. B., Jura, M., & Loewenstein, M. 1983, ApJ, 270, 88

Jenkins, E. B., & Shaya, E. J. 1979, ApJ, 231, 55

Morton, D.C. 1991, ApJS, 77, 119

Mullman, K. L., Lawler, J. E., Zsargó, J., & Federman, S. R. 1998, ApJ, 500, 1064

Tayal, S. S. 1998, ApJ, 497, 493

Wannier, P., Andersson, B-G, Penprase, B.E., & Federman, S.R. 1999, ApJ, 510, 291

Welty, D. E., & Hobbs, L. M. 2000, ApJ, in press

Welty, D. E., Hobbs, L. M., & Kulkarni, V. P. 1994, ApJ, 436, 152

Welty, D. E., Hobbs, L. M., Lauroesch, J. T., Morton, D. C., Spitzer, L., & York, D. G. 1999, ApJS, 124, 465

Wiese, W., Fuhr, J., & Deters, T. M. 1996, *Atomic transition probabilities of carbon, nitrogen, and oxygen : a critical data compilation.*, Ed. W.L. Wiese, J.R. Fuhr, and T.M. Deters, (Washington, DC : American Chemical Society)

Zsargó, J., & Federman, S. R. 1998, ApJ, 498, 256

Zsargó, J., Federman, S. R., & Cardelli, J. A. 1997, ApJ, 484, 820

Zsargó, J., Federman, S. R., & Welty, D. E. 2001, in preparation

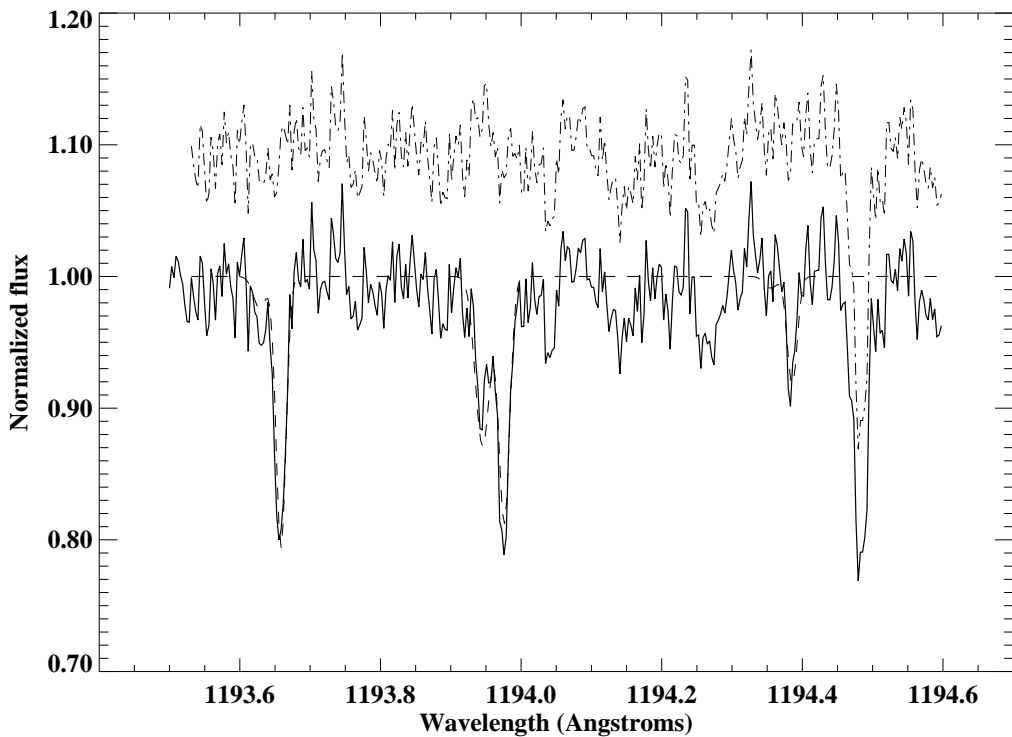


Fig. 1.— High Resolution spectra of multiplet  $\lambda 1194$  toward 1 Sco. The solid and dashed lines are the observed and the calculated spectra, respectively, and the dash-dotted line shows the residuals (offset to +1.1). The Si II line at  $1194.5 \text{ \AA}$  was not synthesized.

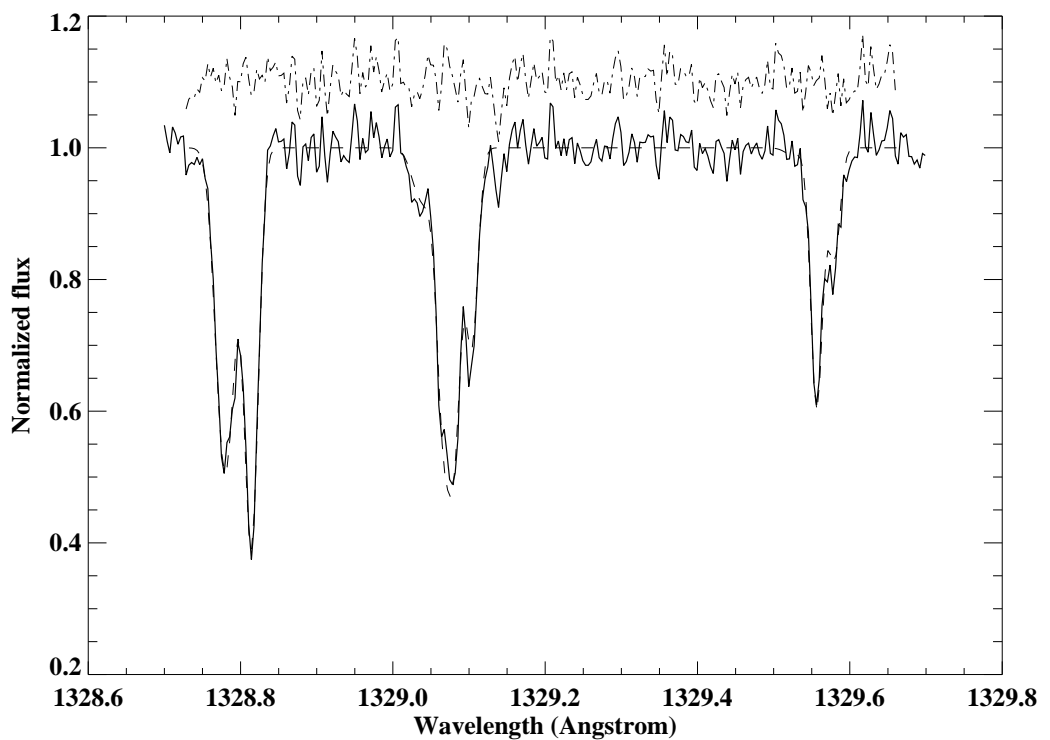


Fig. 2.— High resolution spectra of multiplet  $\lambda$ 1329 toward 1 Sco. The definition of the line types is the same as in Fig 1.

**Table 1: Observations**

Archival code	Range (Å)	Date of observation	Grating (aperture)
$\lambda$ Ori			
z3di0204t	1157–1164	01/23/97	Ech-A (LSA)
z3di0205t	1158–1164	01/23/97	Ech-A (LSA)
z2c20306t	1226–1265	09/14/94	G160M (SSA)
z2c20307t	1230–1266	09/14/94	G160M (SSA)
z2c20308t	1231–1267	09/14/94	G160M (SSA)
z2520306t	1316–1352	02/19/94	G160M (SSA)
z2520307t	1326–1362	02/19/94	G160M (SSA)
z2520308t	1327–1363	02/19/94	G160M (SSA)
1 Sco			
z2zx020bp	1327–1334	03/14/96	Ech-A (SSA)
z2zx020fp	1188–1195	03/14/96	Ech-A (SSA)
z0zi0708m	1114–1150	07/26/92	G160M (SSA)
z0zi070bm	1229–1265	07/26/92	G160M (SSA)
z0zi070ct	1270–1306	07/26/92	G160M (SSA)
z0zi070dt	1325–1361	07/26/92	G160M (SSA)
z0zi070gt	1534–1569	07/26/92	G160M (SSA)
z0zi070it	1644–1679	07/26/92	G160M (SSA)
$\delta$ Sco			
z3di0504t	1157–1163	08/20/96	ECH-A (LSA)
z3di0505t	1158–1164	08/20/96	ECH-A (LSA)
z34r020dt	1254–1261	03/04/96	ECH-A (SSA)
z34r020et	1255–1262	03/04/96	ECH-A (SSA)
z2c20506t	1228–1265	04/23/94	G160M (SSA)
z2c20507t	1231–1267	04/23/94	G160M (SSA)
z2c20508t	1231–1267	04/23/94	G160M (SSA)

Table 2:  $W_\lambda$  of neutral carbon lines toward  $\lambda$  Ori

$\lambda$ (Å)	Measured (mÅ)		Other Measurements		Calculated (mÅ)
	HR <sup>a</sup>	MR <sup>a</sup>	JS <sup>b</sup>	JJL <sup>c</sup>	
<b>J = 0:</b>					
1157.910A <sup>d</sup>	26.97 $\pm$ 0.26	...	...	...	28.09
1157.910B <sup>d</sup>	2.59 $\pm$ 0.30	...	...	...	4.25
1158.324A	15.28 $\pm$ 0.23	...	...	...	15.52
1158.324B	2.99 $\pm$ 0.35	...	...	...	1.52
1260.736A	...	35.44 $\pm$ 0.33	37.0 <sup>e</sup> $\pm$ 2.0	38.0 <sup>e</sup> $\pm$ 2.6	31.27
1260.736B	...	3.17 $\pm$ 0.24	...	...	4.88
1328.833	...	48.23 $\pm$ 0.32	52.0 <sup>e</sup> $\pm$ 4.0	51.0 <sup>e</sup> $\pm$ 2.6	45.66
<b>J = 1:</b>					
1157.770	5.82 $\pm$ 0.21	...	...	...	5.58
1158.035	8.95 $\pm$ 0.21	...	...	...	9.56
1158.130	4.42 <sup>f</sup> $\pm$ 0.21	...	...	...	4.28
1158.674	0.85 $\pm$ 0.09	...	...	...	1.25
1158.732	1.39 $\pm$ 0.10	...	...	...	1.47
1260.927	...	5.17 $\pm$ 0.22	...	$\leq$ 6.3	8.71
1260.996	...	9.55 $\pm$ 0.36	...	6.3 $\pm$ 2.1	6.84
1261.122	...	9.73 $\pm$ 0.30	13.0 $\pm$ 1.0	7.6 $\pm$ 2.1	10.43
1329.085	...	...	...	...	12.96
1329.100	...	47.83 <sup>g</sup> $\pm$ 0.32	42.0 <sup>g</sup> $\pm$ 2.0	56.0 <sup>g</sup> $\pm$ 3.0	15.25
1329.123	...	...	...	...	10.39
<b>J = 2:</b>					
1158.019	2.15 $\pm$ 0.21	...	...	...	4.03
1158.132	...	...	...	...	0.44
1158.397	0.87 $\pm$ 0.21	...	...	...	0.74
1261.426	...	1.95 $\pm$ 0.29	3.4 <sup>h</sup> $\pm$ 1.2	$\leq$ 6.3	1.45
1261.552	...	4.82 $\pm$ 0.32	...	$\leq$ 6.6	4.17
1329.578	...	11.68 <sup>i</sup> $\pm$ 0.32	14.0 <sup>i</sup> $\pm$ 2.0	9.5 <sup>i</sup> $\pm$ 3.7	6.60
1329.601	...	...	...	...	2.34

<sup>a</sup> HR: High Resolution spectra, MR: Medium Resolution spectra.

<sup>b</sup> Jenkins & Shaya (1979).

<sup>c</sup> Jenkins et al. (1983).

<sup>d</sup> A: Main component B: Secondary component, if resolved.

<sup>e</sup> Involves both the main and secondary  $J = 0$  components.

<sup>f</sup> Involves a  $\lambda$ 1158.132 ( $J = 2$ ) line.

<sup>g</sup> Total  $W_\lambda$  of  $\lambda\lambda$ 1329.085, 1329.100, 1329.123 lines.

<sup>h</sup> Total  $W_\lambda$  of  $\lambda\lambda$ 1261.426, 1261.552 lines.

<sup>i</sup> Total  $W_\lambda$  of  $\lambda\lambda$ 1329.578, 1329.601 lines.

Table 3:  $W_\lambda$  of neutral carbon lines toward 1 Sco

$\lambda$ (Å)	Measured (mÅ)		Other measurement JJL <sup>b</sup>	Calculated (mÅ)
	HR <sup>a</sup>	MR <sup>a</sup>		
<b>J = 0:</b>				
1193.031A <sup>c</sup>	10.43 ± 0.62	...	...	9.35
1193.031B	11.46 ± 0.62	...	...	9.56
1193.996A <sup>d</sup>	3.63 ± 0.42	...	...	3.62
1193.996B <sup>d</sup>	3.02 ± 0.62	...	...	3.37
1260.736	...	19.73 <sup>e</sup> ± 0.98	22.0 <sup>e</sup> ± 2.4	20.18 <sup>e</sup>
1277.245	...	69.20 <sup>f</sup> ± 1.42	...	37.48 <sup>e</sup>
1280.135A	...	7.38 ± 0.70	...	7.11
1280.135B	...	7.06 ± 0.73	...	6.94
1328.833A	12.97 ± 0.66	14.50 ± 0.86	34.0 <sup>e</sup> ± 4.4	13.98
1328.833B	15.82 ± 0.98	14.50 ± 0.85	...	15.23
1560.309A	...	26.72 ± 0.83	...	21.13
1560.309B	...	14.15 ± 0.75	...	25.06
1656.928A	...	37.89 ± 0.97	...	28.11
1656.928B	...	28.58 ± 0.90	...	37.20
<b>J = 1:</b>				
1193.009 <sup>c</sup>	2.89 ± 0.46	...	...	10.35
1193.679	4.19 ± 0.52	...	...	4.21
1194.406	1.46 ± 0.37	...	...	1.67
1260.927	...	5.23 ± 0.94	≤ 6.6	5.85
1260.996	...	3.45 ± 0.78	≤ 6.6	4.57
1261.122	...	5.11 ± 0.81	≤ 6.0	7.05
1277.513 <sup>g</sup>	...	4.75 ± 1.15	...	9.76
1279.890	...	5.56 ± 0.74	...	6.23
1280.597	...	2.20 ± 0.90	...	3.39
1329.085	6.59 ± 0.52	...	...	8.82
1329.100	9.26 ± 0.56	26.90 <sup>h</sup> ± 1.10	38.0 <sup>h</sup> ± 3.3	10.47
1329.123	7.05 ± 0.63	...	...	7.01
1560.682	...	32.4 <sup>i</sup> ± 0.98	...	23.87
1560.709	...	...	...	12.07
1656.267	...	25.89 ± 0.93	...	25.70
1657.379	...	19.09 ± 0.86	...	19.42
1657.907	...	22.75 ± 0.94	...	22.96

Table 3:  $W_\lambda$  of neutral carbon lines toward 1 Sco continued

$\lambda$ (Å)	Measured (mÅ)		Other measurement JJL <sup>b</sup>	Calculated (mÅ)
	HR <sup>a</sup>	MR <sup>a</sup>		
<b>J = 2:</b>				
1261.426	...	1.20 $\pm$ 0.94	$\leq$ 6.3	2.11
1261.552	...	3.68 $\pm$ 0.68	$\leq$ 6.3	5.41
1277.550 <sup>g</sup>	...	13.07 $\pm$ 0.87	...	10.89
1277.723	...	1.80 $\pm$ 0.89	...	3.05
1280.333	...	2.50 $\pm$ 0.90	...	3.09
1329.578	6.76 $\pm$ 0.55	10.30 <sup>j</sup> $\pm$ 0.94	$\leq$ 8.7	7.91
1329.601	4.63 $\pm$ 0.72	...	...	3.30
1561.340	...	3.26 $\pm$ 0.67	...	3.78
1561.438	...	13.08 $\pm$ 0.81	...	13.42
1657.008	...	15.43 $\pm$ 0.75	...	18.04
1658.121	...	8.99 $\pm$ 0.68	...	9.91

<sup>a</sup> HR: High Resolution spectra, MR: Medium Resolution spectra.

<sup>b</sup> Jenkins et al. (1983).

<sup>c</sup> Blended lines.

<sup>d</sup> A: Main component B: Secondary component, if resolved.

<sup>e</sup> Involves both the main and secondary  $J = 0$  components.

<sup>f</sup> Involves a second component and  $\lambda$ 1277.282.

<sup>g</sup> Blended lines.

<sup>h</sup> Total  $W_\lambda$  of  $\lambda\lambda$ 1329.085, 1329.100, 1329.123 lines.

<sup>i</sup> Total  $W_\lambda$  of  $\lambda\lambda$ 1560.682, 1560.709 lines.

<sup>j</sup> Total  $W_\lambda$  of  $\lambda\lambda$ 1329.578, 1329.601 lines.

Table 4:  $W_\lambda$  of neutral carbon lines toward  $\delta$  Sco

$\lambda$ (Å)	Measured (mÅ)		Other measurement JS <sup>b</sup>	Calculated (mÅ)
	HR <sup>a</sup>	MR <sup>a</sup>		
<b>J = 0:</b>				
1157.910A <sup>c</sup>	23.06 ± 0.28	...	...	20.36
1157.910B <sup>c</sup>	2.11 ± 0.20	...	...	4.87
1158.324A	10.84 ± 0.23	...	...	10.78
1158.324B	1.44 ± 0.25	...	...	1.89
1260.736A	21.46 ± 0.43	28.53 <sup>d</sup> ± 0.22	32.0 <sup>d</sup> ± 3.0	22.72
1260.736B	6.03 ± 0.36	...	...	5.56
<b>J = 1:</b>				
1157.770	5.06 ± 0.21	...	...	5.38
1158.035 <sup>e</sup>	7.98 ± 0.21	...	...	8.51
1158.130 <sup>f</sup>	4.05 ± 0.22	...	...	4.24
1158.674	1.37 ± 0.14	...	...	1.32
1158.732	1.59 ± 0.13	...	...	1.53
1260.927	7.63 ± 0.30	8.00 ± 0.20	...	7.99
1260.996	6.54 ± 0.31	6.50 ± 0.19	7.2 ± 1.0	6.49
1261.122	8.15 ± 0.31	8.80 ± 0.21	9.7 ± 2.0	9.27
<b>J = 2:</b>				
1158.019 <sup>e</sup>	4.06 ± 0.26	...	...	3.94
1158.132 <sup>f</sup>	0.43 ± 0.22	...	...	0.49
1158.397	0.81 ± 0.21	...	...	0.81
1261.426	1.61 ± 0.30	2.74 ± 0.26	...	1.55
1261.552	3.87 ± 0.35	4.95 ± 0.21	4.6 ± 1.4	4.09

<sup>a</sup> HR: High Resolution spectra, MR: Medium Resolution spectra.

<sup>b</sup> Jenkins & Shaya (1979).

<sup>c</sup> A: Main component B: Secondary component, if resolved.

<sup>d</sup> Involves both the main and secondary  $J = 0$  components.

<sup>e</sup> Blended lines.

<sup>f</sup> Blended lines.

Table 5: Derived parameter values

	Doppler shift (km s <sup>-1</sup> )	Column density (cm <sup>-2</sup> )	<i>b</i> -value (km s <sup>-1</sup> )
$\lambda$ Ori			
Component I.			
J= 0	-0.11	$1.33 \times 10^{14}$	3.02
J= 1	0.28	$5.52 \times 10^{13}$	2.35
J= 2	-1.05	$9.24 \times 10^{12}$	2.50
Component II.			
J= 0	-12.11	$9.55 \times 10^{12}$	3.00
J= 1	-12.11	$1.72 \times 10^{12}$	3.00
J= 2	-12.11	$1.43 \times 10^{12}$	3.00
1 Sco			
Component I.			
J= 0	0.61	$2.49 \times 10^{13}$	1.82
J= 1	0.49	$3.31 \times 10^{13}$	1.48
J= 2	0.01	$1.61 \times 10^{13}$	1.23
Component II.			
J= 0	-7.13	$2.21 \times 10^{13}$	3.05
J= 1	-7.13	$4.32 \times 10^{12}$	2.49
J= 2	-7.13	$3.96 \times 10^{11}$	2.50
$\delta$ Sco			
Component I.			
J= 0	-0.01	$8.87 \times 10^{13}$	2.32
J= 1	0.03	$5.78 \times 10^{13}$	1.19
J= 2	0.14	$1.19 \times 10^{13}$	1.16
Component II.			
J= 0	-4.76	$1.25 \times 10^{13}$	1.41
J= 1	-4.76	$3.82 \times 10^{12}$	1.50
J= 2	...	$\leq 6.72 \times 10^{11}$	...

Table 6: Revised neutral carbon oscillator strengths

$\lambda$ (Å)	Lower	Upper	$f(\text{ZsF})^a$	$f(\text{ZsFC})^b$	$f(\text{M})^c$	$f(\text{H})^d$	$f(\text{WFD})^e$	$f(\text{W})^f$	$\frac{f(\text{M})}{f(\text{ZsF})}$
	State	State	$\times 10^{-3}$						
1194.406	$^3P_1$	$5s\ ^3P_0^o$	3.70(1.01) <sup>g</sup>	...	3.14	3.32	3.19	...	0.85
1193.996	$^3P_0$	$5s\ ^3P_1^o$	12.8(2.9)	14.2	9.41	13.3	12.8	...	0.66
1193.679	$^3P_1$	$5s\ ^3P_2^o$	10.1(1.6)	9.00	3.92	10.6	10.2	6.44	0.39
1193.031	$^3P_0$	$4d\ ^3D_1^o$	41.1(4.8)	54.8	44.5	41.0	45.1	...	1.08
1193.009	$^3P_1$	$4d\ ^3D_2^o$	30.9(5.8)	46.8	33.4	26.4	29.1	...	1.08
1158.732	$^3P_1$	$5d\ ^3F_2^o$	2.23(0.29)	...	1.88	...	...	...	0.84
1158.674	$^3P_1$	$6s\ ^3P_0^o$	1.90(0.27)	...	1.14	...	1.86	...	0.60
1158.397	$^3P_2$	$6s\ ^3P_2^o$	5.91(1.64)	...	2.57	...	4.18	...	0.43
1158.324	$^3P_0$	$6s\ ^3P_1^o$	13.7(2.8)	11.1	3.42	...	5.57	...	0.25
1158.132	$^3P_2$	$5d\ ^3D_2^o$	3.53(1.84)	...	3.27	...	3.66	...	0.93
1158.130	$^3P_1$	$5d\ ^3D_1^o$	6.97(0.79)	1.90	5.44	...	6.09	...	0.78
1158.035	$^3P_1$	$6s\ ^3P_2^o$	17.8(1.8)	...	1.43	...	2.32	...	0.08
1158.019	$^3P_2$	$5d\ ^3D_3^o$	34.0(4.0)	6.41	18.3	...	20.5	...	0.54
1157.910	$^3P_0$	$5d\ ^3D_1^o$	40.5(5.6)	15.6	21.8	...	24.4	...	0.54
1157.770	$^3P_1$	$5d\ ^3D_2^o$	9.36(1.01)	5.71	16.3	...	18.3	5.79	1.74

<sup>a</sup> Present compilation.

<sup>b</sup> Zsargó et al. (1997), with corrections to  $f$ -values for  $J=0$  lines as noted in the text.

<sup>c</sup> Morton (1991).

<sup>d</sup> Hibbert et al. (1993).

<sup>e</sup> Wiese et al. (1996).

<sup>f</sup> Welty et al. (1999); only suggested changes to  $f$ -values of Wiese et al. and Morton are listed.

<sup>g</sup> 1- $\sigma$  uncertainties given in parentheses.